

Received: 25 July 2023 / Accepted: 17 November 2023 / Published online: 20 November 2023

*machine tool thermal error,
correlative compensation model,
ambient effects, ETVE*

Christian NAUMANN^{1*}

Alexander GEIST²

Matthias PUTZ³

HANDLING AMBIENT TEMPERATURE CHANGES IN CORRELATIVE THERMAL ERROR COMPENSATION

Thermal errors are one of the leading causes for positioning inaccuracies in modern machine tools. These errors are caused by various internal and external heat sources and sinks, which shape the machine tool's temperature field and thus its deformation. Model based thermal error prediction and compensation is one way to reduce these inaccuracies. A new composite correlative model for the compensation of both internal and external thermal effects is presented. The composite model comprises a submodel for slow long- and medium-term ambient changes, one for short-term ambient changes and one for all internal thermal influences. A number of model assumptions are made to allow for this separation of thermal effects. The model was trained using a large number of FE simulations and validated online in a five-axis machine tool with measurements in a climate chamber. Despite the limitations, the compensation model achieved good predictions of the thermal error for both normal ambient conditions (21°C) and extreme ambient conditions (35°C).

1. INTRODUCTION

Thermal effects are one of the main causes of positioning errors in machine tools. They are caused by shifting temperature distributions in the machine tool, which lead to thermo-elastic deformations. These temperature fields are shaped by heat sources and sinks, such as waste heat from the cutting process, friction from guides and bearings, power loss from motors, coolants and the environment. Other relevant factors, which influence the time-dependent temperature distribution inside a machine tool, are the heat transfer coefficients and the thermal capacity, which influence the rate at which heat is transferred and stored. It is this multitude of influences that makes thermal issues so difficult to handle.

Categorizing thermal effects can be done by dividing them into internal and external effects. Internal effects are mainly friction, electrical losses, heat from hydraulic and pneumatic units and the cooling system. External effects are mainly conduction with the foundation, convection with the surrounding air, which can be both free or forced convection,

¹ Automation and Monitoring, Fraunhofer IWU Chemnitz, Germany

² Machine Tools, Fraunhofer IWU Chemnitz, Germany

³ IWP, Production Systems and Processes, Chemnitz University of Technology, Germany

* E-mail: christian.naumann@iwu.fraunhofer.de

<https://doi.org/10.36897/jme/175397>

and radiation, e.g. from the sun or from other machines or heat sources. Finally, there are some effects such as process heat, the workpiece, chips and external cooling or lubricating fluids, which may be considered either internal or external.

The distinction between internal and external effects is important because it determines how they may be treated. Internal effects are usually unavoidable consequences of machine tool operation. This is both good, as it makes them somewhat predictable, and bad, as any thermal error compensation strategy inevitably has to deal with them. External influences are usually situational. On the one hand, this means that they are less predictable, but on the other hand, it also means that they can be controlled externally. Examples of this are that using air conditioning can keep the ambient temperature constant, direct exposure to sunlight can be prevented and the workpiece can be tempered to match the machine tool table.

Another important distinction is that internal heat sources usually induce rather large amounts of heat locally with a small delay between cause (e.g. waste heat from a motion) and effect (thermo-elastic deformation). External heat sources or sinks, on the other hand, mostly affect large sections of the machine tool with a small but steady heat exchange over longer periods of time and with a large delay.

Since internal influences are usually local, their effects are often also local and do not necessarily have a large impact on the positioning accuracy. This is however not generally the case, since even a very localized deformation in the wrong part of the machine tool can have a leverage effect on the tool centre point (TCP) and thus become significant. External influences, while seemingly weaker, affect large parts of the machine tool and thus, over time, often cause massive thermal errors.

An important exception to these rules are the cooling systems. They are present in most modern machine tools and are often guided by the ambient temperature. Their purpose is to remove the internal waste heat via fluidic channels and thus to keep the machine tool as close to the ambient temperature as possible. Therefore, they are an internal influence with all the properties of an external influence (unpredictable, large-scale, slow, etc.). While they could thus simply be treated as an external influence, the problem remains that the internal influences cannot be considered without also taking the cooling system into account.

Why this distinction between internal and external influences matters and how it can be used to create a comprehensive thermal error compensation will be explained in Chapter 3. Before that, a brief overview of the state of the art in thermal error compensation strategies will be given. According to Bryan, there are two main strategies for dealing with thermal effects [1]. The first is to reduce the thermal effects directly and the second is to predict or measure the thermal error and to compensate it in the machine tool control with an offset.

Important measures for reducing the thermal effects are thermo-symmetric machine tool design, using cooling systems, reducing the waste heat by reducing electrical losses or friction, diverting the heat through latent heat storage devices, optimizing material parameters, using air conditioning, removing chips, etc.

Measuring the thermal error with great accuracy is rarely possible during the cutting operation. This is mainly because the chips, dirt and coolant are detrimental to most measuring devices and the vibrations caused by the cutting operation create additional errors. Alternatively, it is possible to stop the cutting operation regularly and perform a kind of thermal recalibration. This is however very time consuming and depending on the size and

shape of the workpiece often practically impossible. An implementation of this compensation strategy using eddy current sensors was developed by Schäfer in his PhD thesis [2].

Predicting the thermal error can be done with a variety of different models and sensor inputs. Jungnickel has divided them into [3]:

- Correlative compensation strategies,
- Characteristic model based compensation,
- Structure model based compensation.

Correlative compensation refers to finding and using correlations between state variables, e.g. temperature, axis position, local deformation, motor current and the deformation of an assembly or the TCP. The correlations are found using measurements or simulations and are used to formulate a predictive model. Then the current values of the state variables are obtained from sensors or the machine tool control and the model uses them as inputs to estimate the thermal error, which can then be added as an offset to the commanded TCP position. An example of such a model is the feed-forward artificial neural network (ANN) used by Chen et al. [4] or the multiple regression analysis used by Tseng [5], which both mainly use temperature sensors as input variables.

Characteristic models try to reproduce the relationship between cause and effect of thermo-elastic deformations through the use of transfer functions. Essentially, by knowing the rate at which energy enters the system (e.g. waste heat), the rate at which the energy leaves the system (e.g. convection) and the inner properties of the system (e.g. thermal capacity, conductivity), the transient thermal expansion can be predicted for changing inputs (e.g. motor current, ambient temperature). This only requires knowledge of the system behaviour rather than its exact physical structure. An application of this method was described by Brecher et al. [6], where first and second order time delay functions were used to map the rotation speed and the torque of a main spindle and the ambient temperature onto the TCP displacement. A good demonstration of the effectiveness of using transfer functions for modelling both controlled internal heat sources [7] and cooling systems [8] of machine tools was shown by Mares et al..

Structure models use a relatively exact structural representation of the machine tool as a basis. This usually refers to a finite element mesh of the machine tool's CAD model. Using the FEM, FDM or similar methods, the temperature distribution across the entire machine tool along with the resulting local deformations can be computed by numerically solving the corresponding partial differential equations. Examples of this strategy are the lumped capacitance method (LCM) [9] or the Finite Difference Element Method (FDEM) [10].

The thermal stability of a machine tool is ultimately determined by measurements. These have been standardized in the ISO 230-3, which describes the test code for machine tools under thermal effects. It comprises three parts:

- Environmental temperature variation error (ETVE).
- Thermal distortion due to spindle rotation.
- Thermal distortion due to moving linear axes.

For these tests, any installed compensation needs to be active. The tests are performed and evaluated separately to determine the thermal behaviour of the machine tool. Therefore, in order to significantly improve the thermal behaviour of the machine tool, a compensation method has to deal with all of the aforementioned effects.

Compensation strategies, which are designed to handle ambient effects, are especially the characteristic model based compensation (see e.g. [6]) and the structure model based compensation (see e.g. Delbressine [9] or the PhD thesis of Ess [11]). All they need is an ambient temperature sensor and measurements for model parametrization. Particularly the structure model based compensation can theoretically even handle complex ambient conditions like forced convection. This requires the adaptation of the heat transfer coefficients (HTCs), which are boundary conditions of the FE models. Naumann et al. have shown how these HTCs can be obtained through fluid (CFD) simulations for natural and varying forced convection scenarios [12].

A thermo-elastic simulation can therefore theoretically compute any given thermal load case including changing ambient influences. However, that does not mean, that compensation methods based on these simulations can also do that. The first problem is accurate parametrization. HTCs, e.g., can be different for every machine surface and in the case of forced convection even for every part of every surface. Since they cannot be measured directly, determining them, even with CFD simulations is difficult and imprecise. The second problem is that in order to respond to forced convection in a compensation model, the strength and direction of the airflow needs to be known and that is assuming it is even laminar. Since this is impractical, forced convection is usually prevented or ignored, except for the more predictable air flow resulting from moving assemblies. The third and largest problem is the typically unknown initial state. Assuming the ambient temperature has changed, e.g., in the course of a day-night-cycle. If the machine tool is turned off and then on again, then the simulation has no way of knowing what thermal state to start from, which can lead to large approximation errors. An improvement, here, was reached by Ihlenfeldt et al. through online parameter updates with the help of temperature sensors [13]. An online-capable simulation based compensation model constantly observes relevant temperature sensor readings to gage the validity of its model parameters. The parameters are updated as soon as deviations, e.g. due to wear or ambient effects, are detected.

Correlative methods, on the other hand, are generally poorly suited to deal with ambient temperature changes, since most of them do not consider time as variable. There are, however, some notable exceptions. Yang and Ni [14] used a feed-backward ANN to model a time delay. Naumann and Priber [15] included ambient effects in a high-dimensional characteristic diagram. The idea behind this is that if the environment affects the machine tool, then sensors inside the structure can detect the change. Therefore, given enough, well-distributed temperature sensors and a large enough set of training data, all thermal machine tool states can be approximated, whether they are influenced by internal or external sources. While this solves the problem in theory, in practice, especially for complex machine tools, the number of sensors necessary can become impractical and creating the required training data too costly.

A new method called thermal adaptive learning control (TALC), which uses an autoregressive model with exogeneous inputs (ARX), was developed by the teams of Blaser [16] and Mayr [17]. The ARX model uses both current and past data and can thus handle time-delayed correlations. This ability makes it suitable for handling both ambient and internal effects, which has been demonstrated by Lang et al. [18], who achieved a volumetric error reduction of around 72%. The TALC model uses intermittent displacement measurements to recalibrate itself, as soon as larger accuracy losses are detected.

Beside TALC, recurrent neural networks (RNN) such as the popular long short-term memory (LSTM) neural networks also allow for computing correlations on different time scales. Ngoc et al. used stacked LSTM models and, for comparison, also gated recurrent unit (GRU) models with power consumptions as input variables [19]. Tests of both model types on the rotary axes of a five-axis machine tool yielded high accuracies of over 70%, though at controlled ambient temperatures between 22°C and 23.5°C. Liu et al. used a different LSTM variant, which includes variational mode decomposition (VMD) to remove the coupling effect of high- and low-frequency data and grey wolf algorithms for hyper-parameter optimization [20]. In their tests on spindle systems, over 75% of the thermal error was compensated, which exceeded the results for VMD-LSTM and basic RNN models.

One additional branch of thermal error compensation is through the measurement of local thermal deformations, e.g. through integrated deformation sensors (IDS). Using geometric kinematic models, these local deformations can be used to calculate the thermal displacement of the TCP. Brecher et al. used this method to reduce the thermal error of a 3-axis machine tool by between 50% and 75% [21]. This method is inherently capable of dealing with all heat sources, including all ambient effects, but it requires a suitable placement of IDS.

To summarize, with the present state of the art, the only way to truly ensure thermal stability under variable ambient conditions is to make sure there are no changes in the ambient conditions, i.e. by using strict air conditioning and preventing any radiation or other situational effects. Otherwise, if an ambient temperature sensor is available and forced external convection is prevented, an FEM simulation based prediction presents a good possibility, provided it is kept running continuously. However, even there, ambient effects from moving machine components, cooling systems and, e.g., air evacuation units for housed machines present great difficulties for both modelling and parametrization. New models, like TALC are very promising, the need for additional measurements as well as the fact that complex load scenarios with large internal and external heat sources have yet to be tested leaves room for further improvements and additional research.

Chapter 2 describes a new correlative method of predicting ambient temperature variations. Chapter 3 validates this new method using a case study of the DMU 80 evo five axis machining centre. Finally, a conclusion and outlook on future research will be given.

2. MODELLING AMBIENT EFFECTS

2.1. MODEL ASSUMPTIONS AND SIMPLIFICATIONS

The problem of dealing with a multitude of both internal and external thermal influences in a united, comprehensive compensation model has been outlined in Chapter one. Using a standard correlative model is therefore only effective in simple applications. Consequently, a new approach is needed for more complex machines or thermal conditions.

The main idea is to simplify the thermal interactions in a way that allows the separation of internal and external thermal effects. They can then be modelled separately and be

superimposed. This will introduce additional modelling errors and thus reduce the prediction accuracy but Chapter 3 shows that this simplified model can still create good approximations.

The necessary assumptions (simplifications) for the suggested model are as follows:

1. The cooling system is an external influence and thus a part of the way that the environment affects the machine tool. This is particularly necessary, if the cooling system is guided by the ambient temperature and it affects large parts of the machine tool structure.
2. Any local temperature increase due to waste heat from internal sources produces the same relative deformation, no matter the current overall thermal state of the machine tool. Thus, a deformation from combined internal and external influences is the sum of its constituents.
3. There is a baseline ambient temperature where in the absence of any heat sources or sinks, the relative deformation (thermal error) of the machine tool is zero across the entire workspace. I.e., the machine tool has been properly calibrated at this baseline temperature.
4. The machine has a temporarily constant base temperature. This base temperature can change slowly from one week or month to next but does not change rapidly. Daily cycles are permitted but they always return to the base temperature after less than one day, except for small long-term changes.

The first is merely a matter of definition. This classification may be different if the cooling system is localized or highly effective at cooling the local heat sources.

The second one is necessary to separate fast, local effects (internal) from slow, global effects (external). It is about superposition and also not strictly true. If, e.g., a strong external influence causes the machine tool to twist or tilt due to constrained thermal stresses, then local deformations may also act in slightly shifted directions and vice versa.

The third one sounds simple but it is usually difficult in practice. During a thermal calibration, the machine tool is necessarily in standby, with occasional machine axis movements. This heat is enough to prevent such a constant baseline temperature. Instead, the thermal calibration is usually performed in a thermo-stable equilibrium. This is why many machine tools have a warm-up phase before they start high-precision cutting operations. Using this thermo-stable equilibrium as a baseline is not a problem for the new model. However, if the model training is to be done with simulations, then that simulation needs to be able to reproduce this thermal state quite accurately in order to avoid significant modelling errors in all subsequent steps.

The fourth is perhaps the most restrictive assumption. In order to estimate the deformation caused by ambient temperature changes, these changes can be continuously tracked using an ambient temperature sensor and e.g. a structure model or a transfer function. A correlative method, however, needs machine-internal temperature sensors for such a prediction. These sensors need to be far enough away from internal heat sources to not be affected by them, because the suggested separation would otherwise not be possible. Unless there is a very large number of these sensors, the only way to ensure a reliable prediction is to limit the possible thermal states of the machine tool to a manageable set of ambient thermal load cases. This restriction is necessary to cope with limited resources, both in terms of sensor coverage and training data. Many applications (machines) will not require this simplification.

2.2. COMPENSATION MODEL STRUCTURE

The proposed thermal compensation model consists of three parts:

1. Baseline ambient temperature model,
2. Short-term ambient temperature model,
3. Internal temperature model.

The first one computes the current baseline ambient temperature using (low pass) filtered historical data. For this temperature, the corresponding deformation is computed.

All three models compute the thermal error for the current thermal state at fixed locations (support points) in the workspace. These support points permit the interpolation of the thermal error to any other location in the workspace for online error compensation. To achieve this spatial coverage, a large number of discrete machine poses are investigated (measured / simulated). In the case of the DMU 80 evo, $3^3 = 27$ machine poses were simulated to cover three support points per machine axis, as shown in Fig. 2. Alternatively, the standard Cartesian axis error parameters can be used to describe the error across the workspace, as is done, e.g. in the ISO 230-3.

Model one accounts for seasonal changes or for regional changes if the machine tool is employed in a different part of the world. This model is very simple, since it uses only a single temperature input and it can be trained using stationary FEM simulations (or measurements). In the case study (see Chapter 3), FEM simulations were used. These simulations were done without any internal thermal influences, not even standby power or any form of cooling. This is important for the correct separation of the error components.

The second model computes the deformations resulting from ambient temperature changes that occur in the span of several hours or the course of a day. This model is trained using a number of heating and cool-down cycles with different ambient loads. The models used are hybrid models combining pure regression models (e.g. polynomials or piecewise multilinear models) with transfer functions. Since the inputs are temperature sensors, the transfer functions are applied directly to the input values to create time delays and thereby obtain stronger correlations with the elastic deformations for the subsequent regression models. The optimal combination of input variables, time delays and regression model type varies with each machine tool and often even with different workspace support points.

In Section 2.1, it was mentioned that assumption four is not always needed. In that case, models one and two are combined into a single model for all ambient loads, no matter whether they occur slowly over weeks or more quickly in the span of hours. While this would generally reduce the modelling error, the approximation would also be more complex because more thermal load cases would have to be mapped by a single model. Perhaps even more importantly, without the separation, these heating and cool-down cycles would need to be repeated for many different initial ambient temperatures. The simulations for this second model were transient FEM simulations with active cooling systems but again without any other internal influences like waste heat from motors and guides. See Chapter 3 and [22] for details on the simulation model and its parametrization and validation measurements.

Model three computes the deformations resulting from internal sources only. The model training is done with different axis loads at a constant ambient temperature. In measurements, this is done by periodically moving from one end of an axis to the other and back at different

speeds and repeating this procedure for both individual axes and combinations of axes. Correspondingly, FEM simulations need to reproduce these heat sources in both power and location as closely as possible. Here too, the separation of thermal effects saves vast amounts of training data, since these internal loads only have to be examined for a single (neutral) ambient state.

This type of composite model requires one set of temperature sensors, which keep track of the internal heat sources and one set of sensors (or at least one) which keep track of ambient changes and are not affected by any internal influences. For the DMU 80 evo, two sensors on the machine bed in the back of the machine tool were used to capture the ambient effects. The remaining seven sensors, which are near the drives or bearings are used for the internal model.

Figure 1 shows the structure and interaction of the three models (modules) as implemented for the DMU 80 evo and how they are used to compute the total relative TCP displacement.

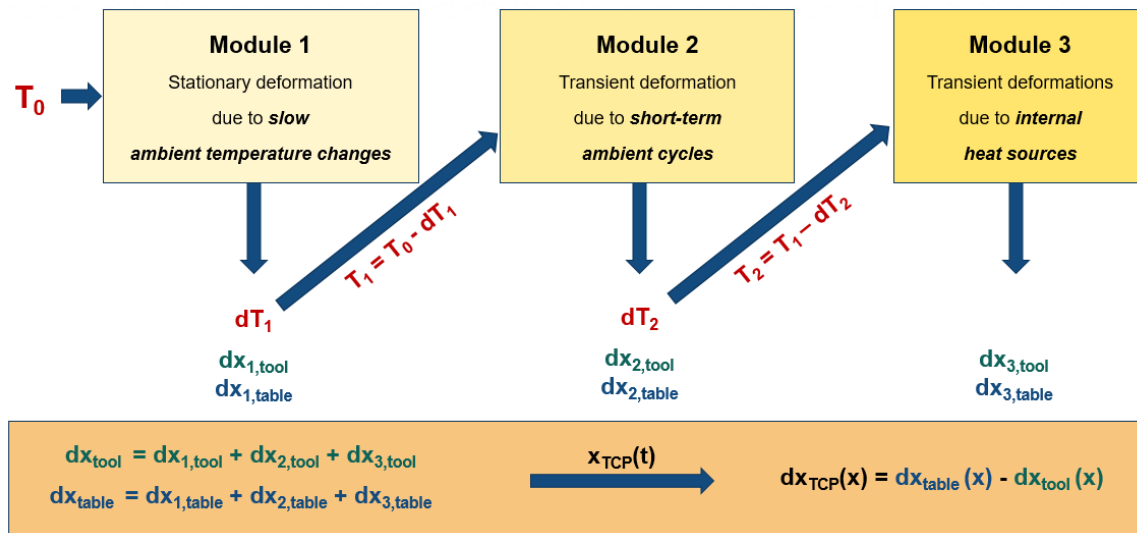


Fig. 1. Composite thermal error compensation model of the DMU 80 evo

In Fig. 1, T_0 is the vector of the current readings of all temperature sensors. Module 1 calculates the thermal error of the machine tool in its current (average) mid-to-long-term ambient state. This disregards internal sources, day-night-cycles and all similar short-term effects. Module 1 receives all temperature readings, but only uses the baseline ambient temperature to compute its portion of the TCP error. On the DMU 80 evo, this baseline temperature is the moving average of sensor T9 (bed 2) over a period of at least three days. Since module 1 only uses a single input, a B-spline can be used to map the displacement on the temperature value. For the DMU 80 evo, the thermal error is computed for the table and tool side separately. This aspect is sensible because not all internal thermal effects affect both error components. Therefore, by separating the error in table and tool side, less process related load cases need to be computed for module 3 and the prediction models have fewer input variables and are thus smaller, simpler and less susceptible to overfitting. Otherwise, this separation is not relevant to the above thermal model structure.

What is also calculated within module 1, is how the mid-to-long term ambient state affects the (internal) temperature sensor readings. In this case, it is sufficient to simply subtract the baseline ambient temperature from all sensor readings. This produces modified temperature sensors readings into a vector T_1 , which holds the inputs for the next layer of the model, see Fig. 1. Module 2 calculates the short-term ambient thermal error and another temperature offset for the internal sensors (here T_1 - T_7 , see Fig. 5). This includes effects from machine tool warm-up, the cooling system and opening the enclosure to exchange workpieces. This offset is represented by the vector dT_2 . The input T_2 needed for the error component corresponding only to internal effects (dx_3) is thus the sensor values T_1 minus this ambient offset dT_2 .

The internal thermal error dx_3 is finally computed in module 3, considering only the internal sources such as motors, guides, bearings and the cutting process. In the end, the different error components, as calculated by the individual models, are added up to produce the total relative error. This model structure requires knowledge of the mid-to-long-term ambient temperature variations. These must therefore be logged in the machine tool control and updated at least periodically. This may be a problem if the machine tool is not in use for longer periods of time. However, in modern production facilities keeping track of the ambient temperature is either already standard practice or else easy to implement.

As mentioned earlier in this chapter, module one uses simple B-splines and modules two and three use combinations of regression models and transfer functions. Alternatively, neural networks could be suitable for this error prediction task. Particularly, time delay neural networks (TDNN) or long short-term memory neural networks (LSTM) could be suitable alternatives for modules two and three. However, if there is little training data to work with, analytical regression models tend to be more reliable.

3. CASE STUDY: THERMAL ERROR COMPENSATION OF THE DMU 80 EVO

The DMU 80 evo is a five-axis vertical machining centre made by DMG Mori. It has a workspace of 800×650×550 mm and a table that can rotate in two axes from a horizontal to a vertical position. In order for the thermal compensation to cover the entire workspace, it was discretized into 27 positions, as shown in Fig. 2. Experience has shown that for the DMU 80 evo, 27 is the minimum number of poses needed to achieve a good interpolation across the workspace. The DMU 80 evo has many cooling channels for removing waste heat from internal sources such as the drives, the spindle or the guides, see Fig. 3. Not shown in Figs. 2 and 3 is the housing, which insulates the machine from external influences while at the same time protecting the operator and the environment from chips and coolant.

Model training was done using FEM simulations, which were parametrized and validated using measurements in a climate chamber [22]. Using such a chamber is not absolutely necessary but it significantly improves the quality of the measurements and thereby the resulting model parametrization. The most important reason for this is that a constant initial temperature of the machine tool can be obtained using the temperature control inside the chamber and FEM simulations generally start from such a constant temperature.

Figure 4 shows the FE mesh used for the simulations. It has around half a million nodes so that transient thermo-elastic simulations can take up to several hours for each load case and machine pose. Therefore, there is an economic limit to how much training data can reasonably be gathered and this affects the complexity limit of any correlative compensation model.

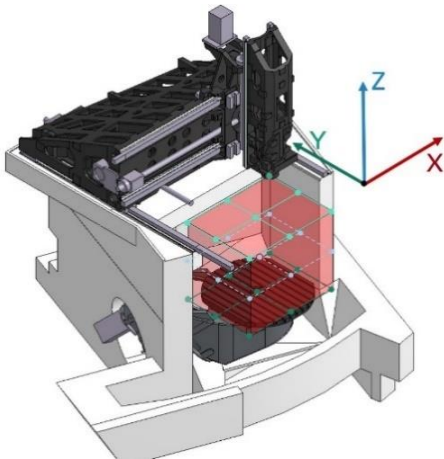


Fig. 2. Workspace of the DMU 80 evo

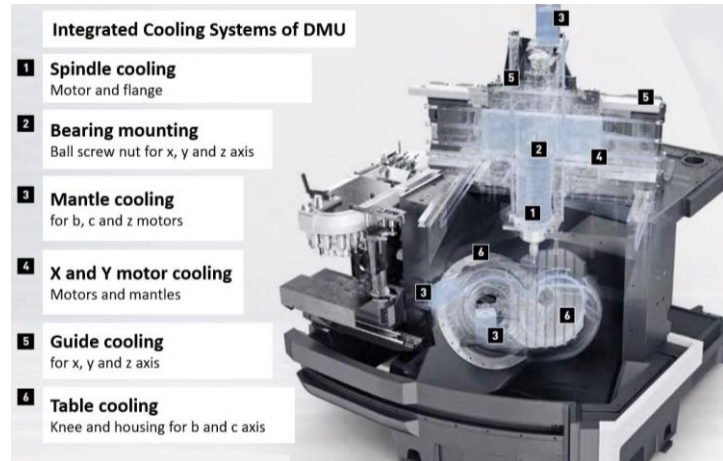


Fig. 3. Cooling systems of the DMU 80 evo [23]

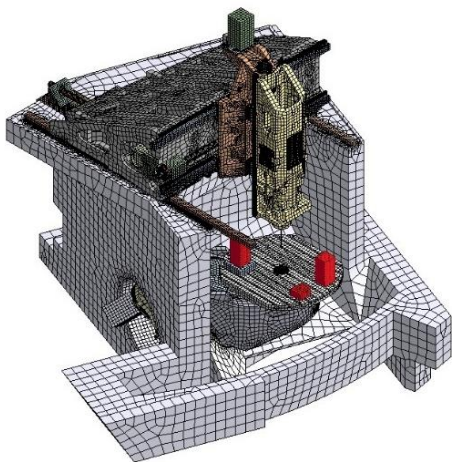


Fig. 4. FE mesh of the DMU 80 evo

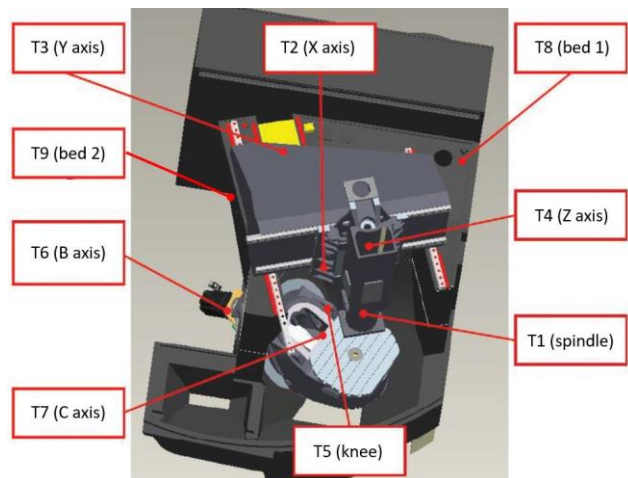


Fig. 5 Temperature sensors of the DMU 80 evo

One of the validation measurements for a load case where all axes were running at rapid feed under constant ambient temperature can be seen in Fig. 6, where dashed lines represent simulated temperatures and solid lines measured temperatures. The dotted red line is the measured room temperature. The locations of the nine temperature sensors used for the compensation are shown in Fig. 5, where sensors $T8$ and $T9$ are used for the ambient models and sensors $T1$ – $T7$ for the internal compensation model. The gray line in Fig. 6, which is at an almost constant 23.8°C is from sensor $T8$ in the rear part of the machine. It represents the temperature of the machine structure away from internal heat sources. It is also the sensor, which guides the cooling system. Fig. 6 also shows the importance of considering the interactions of the cooling system with the thermal state of the machine tool.

Theoretically, sensor T_8 should be at roughly 20.7°C , which is the room temperature. Instead, because the guiding sensor is located near the control cabinet, it is affected by some of its waste heat and therefore almost two degrees higher. The cooling system thus warms the machine tool up even though the ambient temperature is at a constant lower level.

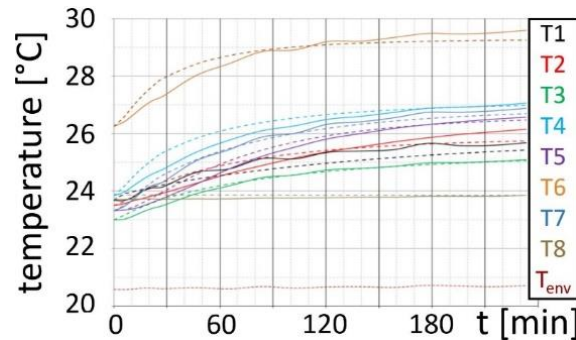


Fig. 6. Simulated vs. measured temperatures

3.1. THERMAL ERROR COMPENSATION MODEL

The general structure of the model was described in Chapter 2.2. In order to cover the entire workspace of the machine tool, the error was separated into a tool component and a table component. The tool component depends on the position of the x -, y - and z -axis. Therefore, the 27 positions shown in Fig. 2 were chosen to cover the workspace. Between these poses, quadratic interpolation ensures a smooth transition. With the interpolation as a separate step, the 27 poses can each be given their own compensation model, which then only depends on temperatures and is independent of the position. While handling such a large number of models is more cumbersome, it reduces the input dimension of the models and thus reduces the chance of overfitting.

The second error component is the table error which is subdivided by the tilt angle into a horizontal ($B=0^\circ$) and a vertical ($B=90^\circ$) position with linear interpolation in between. For more accuracy, further intermediate steps could be added. Finally, the relative TCP error can be calculated by subtracting the tool error from the table error. The table rotation (C -angle) is ignored for three reasons. Firstly, the table deformation is likely similar for all points that are an equal distance from the table center. Secondly, there is only one temperature sensor near the table surface and it is located in the table center. Complex or asymmetrical thermal loads can therefore not be differentiated with this sensor. Thirdly, there is no easy and reliable way to create training data from simulations with different C -angles.

As mentioned in Chapter 2.2, the first model describing the current baseline deformation of the entire machine tool is computed from stationary simulations using a piecewise linear characteristic curve (B-spline). This curve, both the simulated values and the ones predicted by the model, are shown for the TCP error at the central machine pose in Fig. 7. The chart shows, that the stationary deformation of the machine tool with all systems off is linear. It also shows that if all thermal influences were included in a single model, then model errors, e.g. from overfitting due to insufficient training data, could be more than a tenth of a millimetre. Therefore, having a composite model that first takes care of the mid-to-long-term ambient

effects, which are both easier to calculate and overall much larger, significantly enhances the reliability of these regression based models.

Model two, which describes deformations from short-term ambient temperature changes, uses two temperature sensors in the rear of the machine tool which are not affected by internal heat sources. One of these is the previously mentioned sensor *T8*. The other one, sensor *T9*, was additionally installed for this purpose.

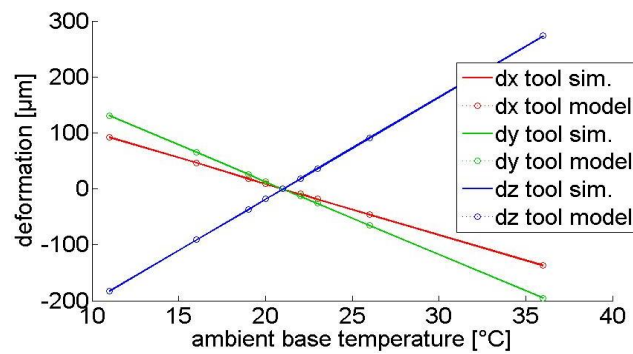


Fig. 7. Deformation prediction ambient model one

The approximation of the internal temperature sensor values, which form the offset vector dT_2 , was done with analytical functions, see equations (1)–(7). The training data was obtained by simulating nine different heating/cooling cycles with ambient temperature differences between -10K and $+15\text{K}$ relative to a reference temperature. For these simulations, the reference temperature was the initial value and had zero deformation. Later, the reference temperature will be the current baseline temperature according to model one. For the nine simulations, the initial state was the constant baseline temperature of 21°C . From this temperature, the ambient temperature was changed for each simulation, first raised to 21.2°C ($+0.2\text{K}$), 22°C ($+1\text{K}$), 23°C ($+2\text{K}$), 26°C ($+5\text{K}$), 36°C ($+15\text{K}$) and then lowered to 20°C (-1K), 19°C (-2K), 16°C (-5K) and finally 11°C (-10K). The ambient temperature change was linear for 2 hours, then kept constant for about a week, followed by a return to the baseline ambient temperature within 2 hours and then again kept constant for another day and a half. Fig. 8 shows the temperatures for the 36°C simulation, which corresponds to simulation 9 (roughly steps 415 to 470 in Fig. 9 and following).

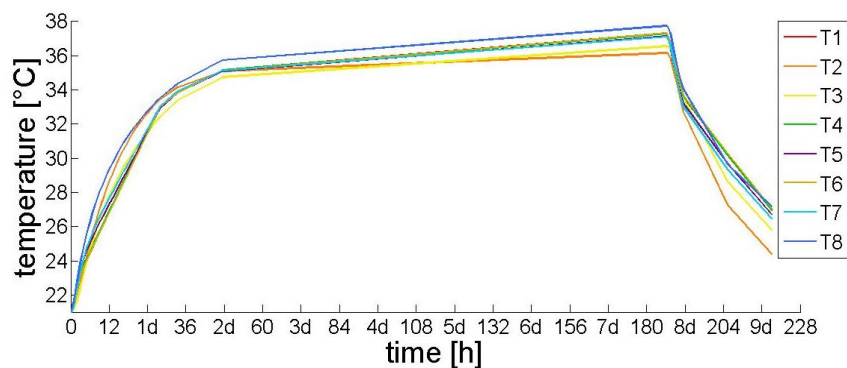


Fig. 8: Simulated temperatures for ambient temperature change 21°C to 36°C

The analytical functions for the temperature offsets dT_2 were obtained by comparing the input and output data, guessing a general function shape and then optimizing the function parameters to obtain the best fit.

The functions are as follows:

$$dT_{2,1} = T_{1,8} - 0.4K + \frac{0.4K^2}{|2 \cdot T_{1,8}| + 1K} \quad (1)$$

$$dT_{2,5} = T_{1,8} - 0.5K + \frac{0.5K^2}{|2 \cdot T_{1,8}| + 1K} \quad (5)$$

$$dT_{2,2} = T_{1,9} - 1K + \frac{1K^2}{(|T_9| - T_{1,9})/3 + 1K} \quad (2)$$

$$dT_{2,6} = T_{1,8} - 0.35K + \frac{0.35K^2}{|2 \cdot T_{1,8}| + 1K} \quad (6)$$

$$dT_{2,3} = T_{1,9} \cdot 1.05 \quad (3)$$

$$dT_{2,7} = T_{1,8} - 0.55K + \frac{0.55K^2}{|2 \cdot T_{1,8}| + 1K} \quad (7)$$

$$dT_{2,4} = T_{1,8} - 0.4K + \frac{1K^2}{|2 \cdot T_{1,8}| + 1K} \quad (4)$$

The inputs are the ambient sensors T_8 and T_9 , which have already been processed by module one (depending on the baseline ambient temperature) to become $T_{1,8}$ and $T_{1,9}$. Both are in degrees Kelvin and in accordance with the load case specifications will generally run between $-10K$ and $+15K$. What this means, is that in a production hall with, e.g. $20^\circ C$, the simulation data would cover potential day-night-cycles in the range of $10^\circ C$ (night) up to $35^\circ C$ (day). Guessing the function types used above, was mainly done by testing $T_{1,8}$ and $T_{1,9}$, choosing the better of the two as dominant input variable and testing different combinations of polynomials and fractions to reduce the residual error. If this is too complicated or not successful, a 1D or 2D characteristic diagram or a neural network should work just as well. The functions only have to look like the simulated displacement within the limited temperature range. They do not have to make sense thermo-dynamically. However, simple analytical functions with as few input variables as possible are generally more reliable. Large gradients should also be avoided, since the use of the ambient baseline temperature in module 1 means that, in practice, $T_{1,8}$ and $T_{1,9}$ will usually be a bit off.

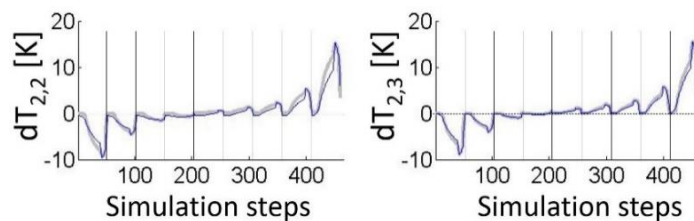


Fig. 9. Temperature offset prediction in ambient model two

Figure 9 shows the simulated temperatures in gray vs. the estimated temperatures in blue for two of the sensors. The graphs contain nine concatenated simulations, where each simulation has changing time steps spanning a total of 220 hours. With the analytical functions (1)–(7), the estimation error is less than one Kelvin for large temperature changes and less than half that for small variations. Though this is both training and test data, the nature of these simple, univariate equations makes overfitting unlikely.

The deformations for model two are likewise mostly approximated using analytical functions. Here, however, the complex interaction between the machine tool, the surrounding

air and the cooling system make the prediction more difficult. For small temperature changes, the ambient temperature has a weak effect compared to the cooling system, which acts as a heat source. For large ambient temperature changes, the cooling system has some effect at the start of the simulations and then less and less. To account for these differences, the model was split into three modes (i.e. temperature ranges). The first one is for small ambient changes ('stable'), the second for large positive changes ('warm') and the third for large negative changes ('cold'), see Fig. 10. While this makes the overall compensation much more cumbersome, it is unavoidable, if simple approximation models are to be used (in the case of the DMU 80 evo). Here, sensor "bed 2" was used to differentiate the submodels. Values of $T_{1,9}$ between -1.6K and $+1.6\text{K}$ count as small changes and all values below or above this interval are modelled separately.

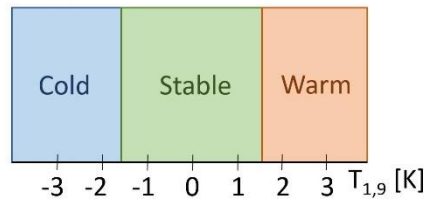


Fig. 10. Temperature ranges for the three displacement submodels of ambient model two

The change from one mode to another was done using equations (8) and (9):

$$s = \max(1 - (T_{1,9}/1.6\text{K})^6; 0) \quad (8)$$

$$dx = \begin{cases} s \cdot dx_{stable} + (1 - s) \cdot dx_{cold}, & T_{1,9} < 0 \\ s \cdot dx_{stable} + (1 - s) \cdot dx_{warm}, & T_{1,9} \geq 0 \end{cases} \quad (9)$$

The scalar s in (8) allows for a smooth transition from one mode to the next and ensures that this transition only occurs near the border of the stable interval. dx in (9) denotes a deformation, such as the tool x displacement.

The actual models can differ for each error component or each position in the workspace. The stable mode, which was the most difficult to approximate, was done using 2D characteristic diagrams with T_8 and T_9 as input variables. Here, some additional improvements were achieved by adding a time delay for the x component of the tool error. Such a delay can be implemented by using temperature inputs from e.g. one hour earlier instead of the current values. A better alternative is, however, to use a very wide (large sigma) one-sided Gaussian filter.

The submodels for the warm and cold temperature ranges were done using analytical functions. An example of this is shown in (10) for the y error of the tool at the second machine pose:

$$dy_{tool,pose_2} = \begin{cases} 9.5 \frac{\mu\text{m}}{\text{K}} \cdot |T_{1,9}|^{1.22}, & \text{cold} \\ \text{char. diagram}, & \text{stable} \\ -22 \frac{\mu\text{m}}{\text{K}} \cdot |T_{1,9}|^{0.82}, & \text{warm} \end{cases} \quad (10)$$

Most of the other equations (x , y and z error for all 27 poses) have a similar structure with merely different factors and exponents. The exception is the x displacement of the tool for positions on the right end of the workspace ($x \approx 400$ mm). There, the deformation has a non-monotonous behaviour. As the ambient temperature increases, the x displacement initially becomes negative and then reverses and becomes positive. This behaviour was modelled as the sum of two opposing PT_1 transfer functions. The corresponding gains and delays were found by testing all possible combinations within a manually defined interval.

Figure 12 shows the approximated tool y displacement for pose 2 using equation (10) and Fig. 11 the x displacement for machine pose 25, which uses PT_1 transfer functions.

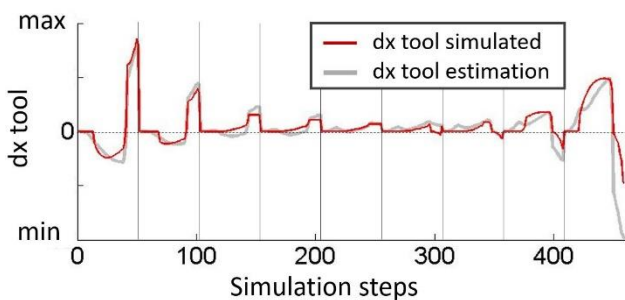


Fig. 11. Deformation prediction x tool pose 25

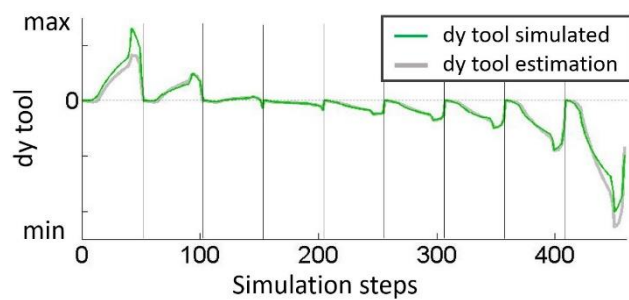


Fig. 12. Deformation prediction y tool pose 2

The graphs in Figs. 11 and 12 show that the approximations are good for the most part but not perfect. In Fig. 11, between steps 100 and 400, the approximations do not follow the deformations very well. This is in part a side effect of the overlapping modes (see eq. (9)). Since the approximation error is still well below $5 \mu\text{m}$, this is, however, acceptable. There are also larger errors in simulations 1 (steps 0 - 55) and 9 (steps 415 - 470), where large ambient temperature changes occur. The corresponding simulations were merely added to improve the extrapolation of the models. Their approximations are worse, because they were given very little consideration during the parameter optimization for the cold and warm submodels. Absolute deformation values in Figs. 11 and following were redacted due to client confidentiality.

In general, the approximations of the tool error's x , y and z components, are nearly perfect, except for slightly larger x errors for the right side of the workspace and larger errors for ambient temperature changes $> \pm 5\text{K}$. Due to the simplicity of these models, the extrapolation to other load cases within this temperature range will likely be similarly good. For the table component of the thermal error, similar approximation models were used.

Model three for the inner heat sources (motors, guides, bearings, etc.) uses a combination of PT_1 elements and characteristic diagrams (i.e. multivariate, piecewise multilinear models) with temperature variables $T_{2,1} - T_{2,7}$ as inputs. Both single axis movements and various combinations of two or more axes at different axis speeds (with and without the use of coolant) were used to train the third compensation model, see [22].

Finally, the deformations from all three models are added to compute the current estimation for all 27 workspace support points. They are then interpolated for the current TCP location using 3D quadratic interpolation to obtain the current value of the TCP error. While the explanations above have focused on the tool error components, the table error uses

the same techniques and model types. In the investigation here, the table error was described by only 10 parameters, specifically a translation (dx , dy , dz) and a tilting (rx , ry) for both the vertical ($B=0^\circ$) and the horizontal table position ($B=90^\circ$). Between these two sets of five parameters each, linear interpolation is used. A more exact method of describing the table error using a characteristic diagram (2D piecewise multilinear surface) of the table surface was developed and tested in [24]. However, this compensation model here can equally be applied to the improved table model, where each support point of the characteristic diagram is considered as one table parameter and receives its own thermal compensation model.

3.2. VALIDATION MEASUREMENTS

To validate the compensation models, two measurements were performed. The first one, at a constant 21°C ambient temperature, lasted around one day and was structured as follows:

- 1 h **production program** with external cutting fluid (ECF), axis movements at cutting speed, spindle at 50% of max. speed,
- 1 h production program without ECF; followed by 1 h cool-down with all axes in stand-by,
- 1 h **mold making program** with ECF, axis movements at 50% of rapid feed, spindle at max. speed,
- 1 h mold making program without ECF; followed by 1 h cool-down with all axes in stand-by,
- 1 h **spindle program** with spindle running at max. speed with ECF, without axis movements,
- 1 h spindle run without ECF; followed by 1 h cool-down with spindle in stand-by,
- 2 h **x-axis** movement with 75% of rapid feed without ECF; followed by 1 h cool-down in stand-by,
- 2 h **y-axis** movement with 75% of rapid feed without ECF; 1 h cool-down,
- 2 h **z-axis** movement with 75% of rapid feed without ECF; 1 h cool-down,
- 2 h **b-axis** movement (table swivel) with 75% of rapid feed without ECF; 1 h cool-down,
- 2 h **c-axis** movement (table rotation) with 75% of rapid feed without ECF; 1 h cool-down.

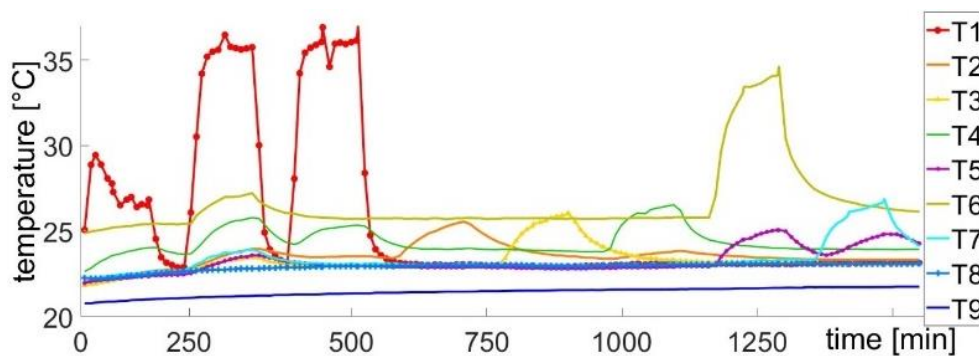


Fig. 13. Temperatures of measurement 1

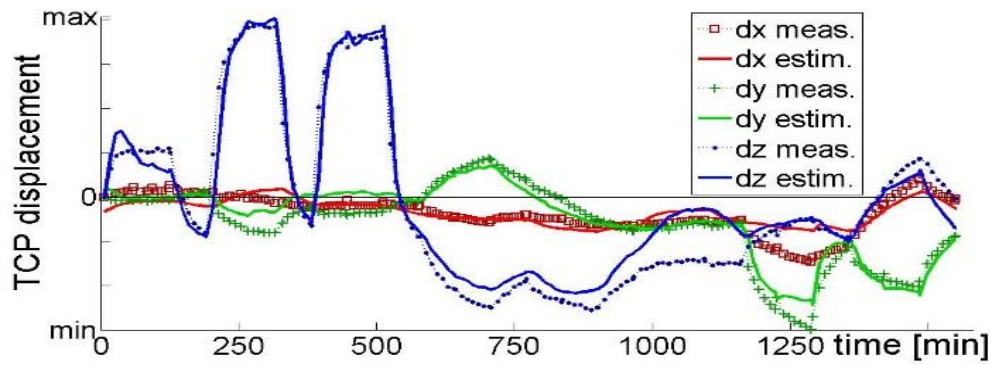


Fig. 14. TCP displacement of probe 2V in measurement 1

The second test load case was performed at 35°C ambient temperature and lasted for about three days and was structured as follows:

- 3.5 h air cutting with **all five axes** at 75% of rapid feed (each axis performs one full move across its axis range in sequence, i.e. only one axis moves at any time), spindle in stand-by, without ECF,
- 3.5 h of the same but with ECF; followed by 3.5 h cool-down with all axes in stand-by,
- 3.5 h air cutting with the **x-axis** at 75% of rapid feed; all other axes/spindle in stand-by, without ECF,
- 3.5 h of the same but with ECF; followed by 3.5 h cool-down with all axes in stand-by,
- 3.5 h air cutting with the **y-axis** at 75% of rapid feed; all other axes/spindle in stand-by, without ECF,
- 3.5 h of the same but with ECF; followed by 3.5 h cool-down with all axes in stand-by,
- 3.5 h air cutting with the **z-axis** at 75% of rapid feed; all other axes/spindle in stand-by, without ECF,
- 3.5 h of the same but with ECF; followed by 3.5 h cool-down with all axes in stand-by
- 3.5 h air cutting with the **b-axis** at 75% of rapid feed; all other axes/spindle in stand-by, without ECF,
- 3.5 h of the same but with ECF; followed by 3.5 h cool-down with all axes in stand-by,
- 3.5 h air cutting with the **c-axis** at 75% of rapid feed; all other axes/spindle in stand-by, without ECF
- 3.5 h of the same but with ECF; followed by 3.5 h cool-down with all axes in stand-by.

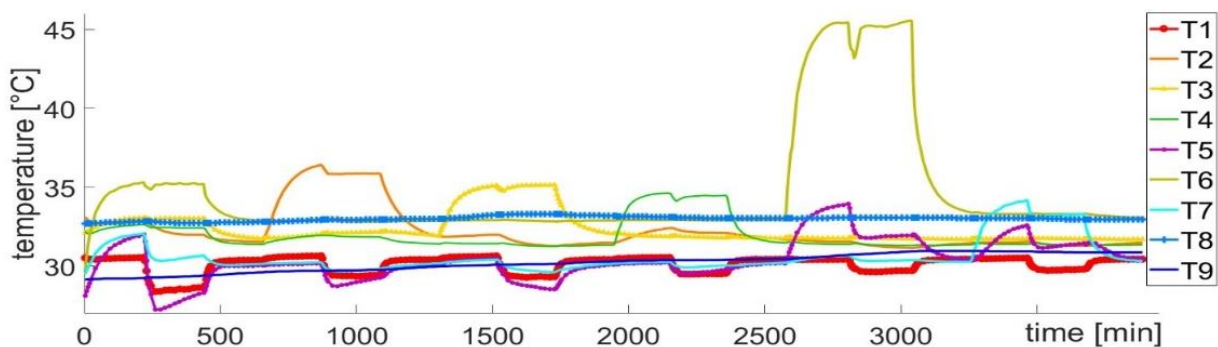


Fig. 15. temperatures of measurement 2

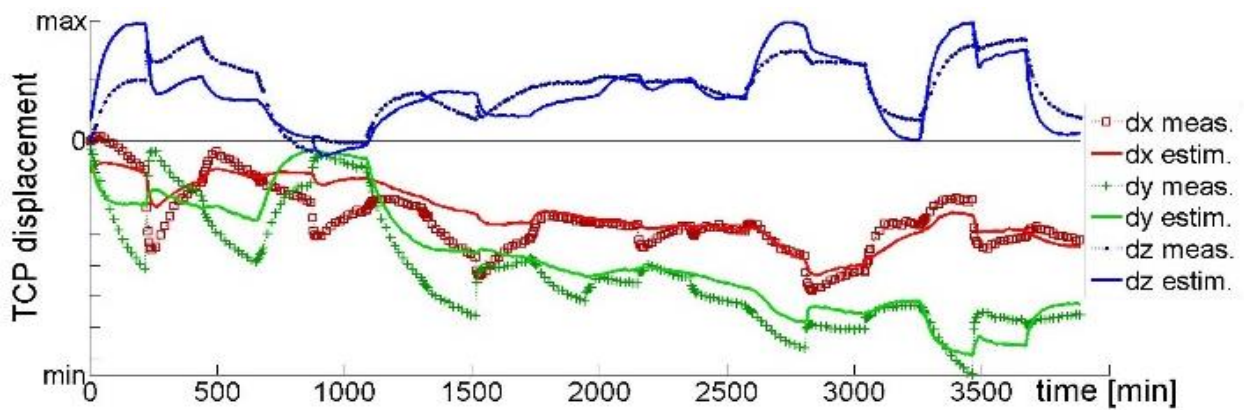


Fig. 16. TCP displacement of probe 3H in measurement 2

The experiments comprised repeated measurements of three locations within the workspace for both the vertical and horizontal table configurations. The validation measurements were done with a touch probe mounted as a tool and three cuboids fixed on the table (see Fig. 4). None of these measurement locations (top corners of the cuboids in Fig. 4) correspond with any of the workspace support points (vertices in Fig. 2) so that the spatial interpolation could also be tested. Figs. 13 and 15 show the temperatures for the two measurements.

Figures. 14 and 16 show the corresponding displacements, both measurements and model predictions. Fig. 14 shows the error of probe 2 in the vertical table position, see Fig. 17. Figure 16 shows the error for probe 3 in the horizontal table position. The root mean square deviation of the relative error for measurement 1 was reduced by 56–72% across the six measurement locations. For measurement 2, the reduction was 42–52%.

While this composite three-part compensation model was created and optimized for the DMU 80 evo and it has some limiting model assumptions, it has proven to be a functioning compensation strategy for thermal errors, despite the complexity of both the machine tool and the investigated internal and external thermal loads.

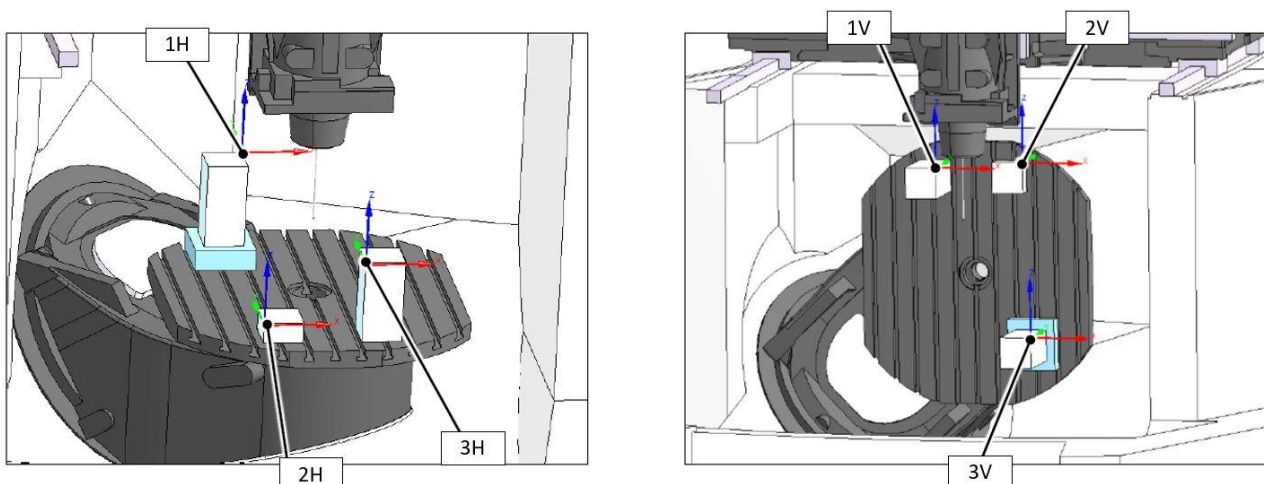


Fig. 17. measurement locations for validation experiments

3.3. MODEL APPLICATION

The presented correlative compensation method has been discussed in terms of motivation, methodology and validation. It remains to examine when such a model can be used and when it should be used.

The main requirement is for the thermal error to be separated into an ambient and an internal component. These components must have significantly different thermal time scales so that they can be superimposed independently with little error. Ideally, the machine tool should have a large thermal capacity and low conductivity. This may, e.g. be problematic for light-weight structures. The best way to test this, is by running three experiments: first an internal load profile at a constant/neutral ambient state, second an ambient load profile without internal loads and thirdly the same ambient load profile with the internal loads from experiment one. This should reveal if there is any chance of superposition.

A secondary requirement is the ability to gather large amounts of data, which means either a validated simulation model and/or access to a climate chamber. Note that the model described here would have been nearly impossible to obtain without FEM simulations due to the large number of necessary training load cases and the need to obtain all deformation data for 27 different locations in the workspace.

Another requirement is the need for several temperature sensors, of which at least one must be independent of internal heat sources and sinks. In some cases, an air temperature sensor may instead be used as input for the ambient model.

When the model should be used is subjective. In the view of the authors, simple unified models (e.g. characteristic diagrams or artificial neural networks) should always be preferred wherever possible. Here the complexity of the machine and its thermal behaviour prevented such simple models. If the skill and computational capabilities allow, a simulation-based compensation may be more effective than correlative strategies. Note that the step from a validated FEM model to a reliable online-capable simulation-based compensation is a very big one. Lastly, if the above requirements are not met and a correlative compensation is still desired, then the best option is to add more temperature sensors and use more training data with both internal and ambient loads in order to create a more complex unified model.

One final aspect to be considered is the typical milling process. Most often, an operator places a workpiece on the machining table, measures its location and then starts the cutting operation with cutting fluid. For the DMU 80 evo, the linear encoders of the translational axes will ensure position-independent accuracy while the cutting fluid minimizes the table error. Therefore, unless the cutting operation takes very long, the error will not depend much on the current ambient thermal machine tool state. What remains are mainly the internal thermal effects from the cutting operation. When using correlative compensation, the presented model is still very useful in this case, since it provides the correct input vector T_2 irrespective of any ambient offsets present in the raw temperature sensor values.

4. SUMMARY AND OUTLOOK

This paper describes and tests a new composite thermal error compensation model for machine tools, which can deal with both internal and external thermal influences.

The compensation method is correlative in nature, as it uses temperature sensors to map the current thermal state directly onto the TCP error. However, it also employs transfer functions to cope with different thermal time scales.

The model consists of three parts. The first one describes long-term ambient changes occurring over weeks or months. The second one describes daily or other short-term ambient cycles. The third one describes the local deformation from all current internal heat sources and sinks. Thermo-elastic FEM simulations were used to compute and study the corresponding thermal effects separately and to train the three models. The compensation models use a combination of regression models (e.g. polynomials and characteristic diagrams) and time delay transfer functions. Validation measurements were performed to show the feasibility of the approach and managed to reduce the thermal error by around 50% for complex internal and external thermal loads.

The next planned steps include a further optimization of the model followed by an online validation measurement. A test of the model during milling operations is also planned. If all tests are successful, a transfer of this method to a different machine type will be attempted.

ACKNOWLEDGEMENT

This research was funded by the German Research Foundation – Project-ID 174223256 – TRR 96, which is hereby gratefully acknowledged.

REFERENCES

- [1] BRYAN J., 1990, *International Status of Thermal Error Research*, CIRP Annals, 39/2, 645–656.
- [2] SCHÄFER W.J., 1993, *Steuerungstechnische Korrektur thermoelastischer Verformungen an Werkzeugmaschinen*, PhD thesis, RWTH Aachen.
- [3] JUNGnickel G., GROSSMANN K., 2006, *Korrektur thermisch bedingter Verformungen an Werkzeugmaschinen mit strukturbasiertem Zustandsmodell*, Proc. 11th Dresdner Werkzeugmaschinen-Fachseminar, 124–135.
- [4] CHEN J.S., YUAN J., NI J., 1996, *Thermal Error Modelling for Real-Time Error Compensation*, International Journal of Advanced Manufacturing Technology, 12, 266–275.
- [5] TSENG P.-C., 1997, *A Real-Time Thermal Inaccuracy Compensation Method on a Machining Centre*, International Journal of Advanced Manufacturing Technology, 13, 182–190.
- [6] BRECHER C., HIRSCH P., WECK M., 2004, *Compensation of Thermo-Elastic Machine Tool Deformation Based on Control Internal Data*, CIRP Annals - Manufacturing Technology, 53/1, 299–304.
- [7] MARES M., HOREJS O., HORNYCH J., KOHUT P., 2011, *Compensation of Machine Tool Angular Thermal Errors Using Controlled Internal Heat Sources*, Journal of Machine Engineering, 11/4, 78–90.
- [8] MARES M., HOREJS O., FIALA S., HAVLIK L., STRITESKY P., 2020, *Effects of Cooling Systems on the Thermal Behaviour of Machine Tools and Thermal Error Models*, Journal of Machine Engineering, 20/4, 5–27, <https://doi.org/10.36897/jme/128144>.
- [9] DELBRESSINE F.L.M. et al, 2005, *Modelling Thermomechanical Behaviour of Multiaxis Machine Tools*, Precision Engineering, 30/1, 47–53.
- [10] MAYR J., et al., 2008, *Simulation and Prediction of the Thermally Induced Deformations on Machine Tools Caused by Moving Linear Axis Using the FDEM Simulation Approach*, Proc. 23rd ASPE Annual Meeting, 168–171.
- [11] ESS M., 2012, *Simulation and Compensation of Thermal Errors of Machine Tools*, PhD thesis, Zurich.
- [12] GLÄNZEL J., IHLENFELDT S., NAUMANN C., PUTZ M., 2018, *Efficient Quantification of Free and Forced Convection via the Decoupling of Thermo-Mechanical and Thermo-Fluidic Simulations of Machine Tools*, Journal of Machine Engineering, 18/2, 41–53, <https://doi.org/10.5604/01.3001.0012.0925>.

- [13] THIEM X., RUDOLPH H., KRAHN R., IHLENFELDT S., FETZER C., MÜLLER J., 2023, *Adaptive Thermal Model for Structure Model Based Correction*, S. Ihlenfeldt (Ed.): ICTIMT 2023, Springer, LNPE, 67–82, https://doi.org/10.1007/978-3-031-34486-2_6.
- [14] YANG H., NI J., 2005, *Dynamic Neural Network Modeling for Nonlinear, Nonstationary Machine Tool Thermally Induced Error*, International Journal of Machine Tools and Manufacture, 45/4–5, 455–465.
- [15] NAUMANN C., PRIBER U., 2012, *Modellierung des Thermo-Elastischen Verhaltens von Werkzeugmaschinen mittels Hochdimensionaler Kennfelder*, Proc. Workshop Computational Intelligence, 22, Dortmund, 365–383.
- [16] BLASER P., PAVLIČEK F., MORI K., MAYR J., WEIKERT S., WEGENER K., 2017, *Adaptive Learning Control for Thermal Error Compensation of 5-axis machine tools*, Journal of Manufacturing Systems, 44/2, 302–309, <https://doi.org/10.1016/j.jmsy.2017.04.011>.
- [17] MAYR J., BLASER P., RYSER A., HERNANDEZ-BECERRO P., 2018, *An Adaptive Self-Learning Compensation Approach for Thermal Errors on 5-axis Machine Tools Handling an Arbitrary Set of Sample Rates*, CIRP Annals, 67, 551–554, <https://doi.org/10.1016/j.cirp.2018.04.001>.
- [18] LANG S., ZIMMERMANN N., MAYR J., WEGENER K., BAMBACH M., 2023, *Thermal Error Compensation Models Utilizing the Power Consumption of Machine Tools*, S. Ihlenfeldt (Ed.): ICTIMT 2023, Springer, LNPE, 41–53, https://doi.org/10.1007/978-3-031-34486-2_4.
- [19] NGOC H.V., MAYER J.R.R., BITAR-NEHME E., 2023, *Deep Learning to Directly Predict Compensation Values of Thermally Induced Volumetric Errors*, Machines, 11, 496, <https://doi.org/10.3390/machines11040496>.
- [20] LIU J., MA C., GUI H., WANG S., 2021, *Thermally-Induced Error Compensation of Spindle System Based on Long Short Term Memory Neural Networks*. Applied Soft Computing, 102, 107094, <https://doi.org/10.1016/j.asoc.2021.107094>.
- [21] BERTAGGIA N., TZANETOS F., ZONTAR D., BRECHER C., 2022, *Investigation of Thermally Induced TCP-Displacement Under Load of the Machine axes in Different Areas*, Procedia CIRP 107, 600-604, <https://doi.org/10.1016/j.procir.2022.05.032>.
- [22] GEIST A., NAUMANN C., GLÄNZEL J., PUTZ M., 2023, *Methods for Determining Thermal Errors in Machine Tools by Thermo-Elastic Simulation in Connection with Thermal Measurement in a Climate Chamber*, MM Science Journal, June 2023, https://doi.org/10.17973/MMSJ.2023_06_2023049.
- [23] DMG MORI, 2019, *DMU eVo-Baureihe*, Document ID P20180411_0419_DE.
- [24] NAUMANN C., NAUMANN A., BERTAGGIA N., GEIST A., GLÄNZEL J., HERZOG R., ZONTAR D., BRECHER C., DIX M., 2023, *Hybrid Thermal Error Compensation Combining Integrated Deformation Sensor and Regression Analysis Based Models for Complex Machine Tool Designs*, S. Ihlenfeldt (Ed.): ICTIMT 2023, Springer LNPE, 28–40, https://doi.org/10.1007/978-3-031-34486-2_3.